Large displacements of light thin flexible structures coupled with heavy fluids using co-simulation between finite element and fast boundary element solvers

Eric Veron, Rabah Bouzidi, Cédric Leblond, Anh Le Van, Jean-François Sigrist

LARGE DISPLACEMENTS OF LIGHT THIN FLEXIBLE STRUCTURES COUPLED WITH HEAVY FLUIDS USING CO-SIMULATION BETWEEN FINITE ELEMENT AND FAST BOUNDARY ELEMENT SOLVERS

Eric VERON *
DCNS Research, 5 rue de l'Halbrane
44 340 Bouguenais, France
eric.veron@dcnsgroup.com
GeM, 2 rue de la Houssinière
44 322 Nantes, France
eric.veron@univ-nantes.fr

Rabah BOUZIDI
GeM - Université de Nantes
2 rue de la Houssinière
44 322 Nantes
France
rabah.bouzidi@univ-nantes.fr

Cédric LEBLOND
DCNS Research
5 rue de l'Halbrane
44 340 Bouguenais
France
cedric.leblond@dcnsgroup.com

Anh LE VAN
GeM - Université de Nantes
2 rue de la Houssinière
44 322 Nantes
France
anh.le-van@univ-nantes.fr

Jean-François SIGRIST
DCNS Research
5 rue de l'Halbrane
44 340 Bouguenais
France
jean-francois.sigrist@dcnsgroup.com

ABSTRACT

This work deals with the dynamic analysis of an immersed circular cylinder, stiffened at its extremities, with a membrane-like behavior subjected to an axial force and fluid-structure interaction loadings. The membrane density and the fluid density are of the same order, hence the added mass effect is significant and the physical coupling is strong. The solution is computed by means of a co-simulation procedure between ABAQUS®/Standard to solve the structural sub-problem and an in-house potential flow code based on boundary integral formulations, to solve internal and external fluid sub-problems. The space coupling, *i.e.* field spatial mapping and field exchanges at the fluid-structure interface, and the time coupling, *i.e.* time synchronization of fluid and structure solvers, are performed using SIMULIA® Co-Simulation Engine. The strong numerical coupling is enforced by using efficient iterative algorithms.

NOMENCLATURE

ρ_F, ρ_S	Fluid and structural density, respectively
g	Gravity
t	Time
$\mathbf{x}$, $\mathbf{y}$	Spatial position
Ω_F	Fluid domain, fluid domain boundary
$\mathbf{n}(\mathbf{x})$	Normal vector on the surface
$\mathbf{v}_m(\mathbf{x})$	Fluid mesh velocity
$G(\mathbf{x},\mathbf{y})$	Green function for a potential problem in an unbounded 3D space
$\phi(\mathbf{x})$	Velocity potential
$\mathbf{v}(\mathbf{x})$	Fluid velocity ($\mathbf{v} = \nabla\phi$)
$p(\mathbf{x})$	Pressure in the fluid domain

INTRODUCTION

The assessment of the dynamic behavior of light thin highly flexible structures coupled with heavy fluids is of paramount importance in biomechanics problems and some ocean energy conversion concepts. This kind of Fluid-Structure Interaction problems highlights two major numerical difficulties. Firstly, the mass ratio is about one and added mass effects due to the kinetic energy of the fluid are of the same order as structural inertial effects. The physical coupling is then strong and the numerical coupling scheme has to be reliable to compute an accurate solution and to ensure that the coupling procedure is stable. Secondly, under external loadings, flexible structures can undergo large displacements, in-

*Address all correspondence to this author.

ducing large topological changes in the fluid domain. The strong physical coupling difficulty, can be circumvented by using implicit coupling schemes such as monolithic algorithms or by means of iterative partitioned algorithms which ensure a converged coupled solution by using an iterative exchange procedure of physical quantities at the fluid-structure interface. Standard Arbitrary Lagrangian Eulerian techniques, which consists in deforming the fluid domain, are not efficient when large displacements of fluid domain boundaries occur as fluid mesh can contain highly distorted elements. Alternative methods have to be used, such as Lagrangian/Eulerian formulation associated with interface capturing algorithms, Lagrangian/Lagrangian formulation by coupling Finite Element and Fluid Particle methods or Lagrangian/Boundary Integral formulation. In the present work, the fluid-structure interaction solution is computed using a co-simulation procedure between the Finite Element commercial code ABAQUS®/Standard to assess the structure behavior and an in-house Fast Boundary Element solver to assess fluid solution and loadings at the fluid-structure interface. The coupling is achieved by means of the ABAQUS® Co-Simulation Engine allowing the user to couple ABAQUS® solvers with a third-party solver. In order to ensure a strong numerical coupling, the standard iterative time coupling scheme available in ABAQUS® is enhanced using relaxation method and Interface Quasi-Newton algorithms which speed up the coupling scheme convergence. The physical problem of interest is an immersed circular elastic membrane cylinder under an axial loading with an internal fluid flow. Circular section at cylinder extremities are highly stiffened with ring shaped structures. Our goal is to assess the structural behavior: non linear large displacements of the membrane, reaction force at membrane extremities and stress level in the membrane. Although the bending stiffness is low, it has a major influence on the wrinkles shape.

STRUCTURAL MODEL

Thin structures with a membrane like behavior, *i.e.* with a very low bending stiffness, can wrinkle when they experience local buckling. This local buckling happens when the thin structure undergoes negative principal stress. Due to this stress cancellation the stiffness matrix tends to be singular and numerical instabilities can occur. The membrane problem is solved by means of the Finite Element commercial software ABAQUS® [1]. The thin membrane is discretized with four nodes shell finite elements (the so-called S4 element from the ABAQUS® finite element library is used). Stiffened extremities of the cylinder are modeled with rigid kinematic constraints.

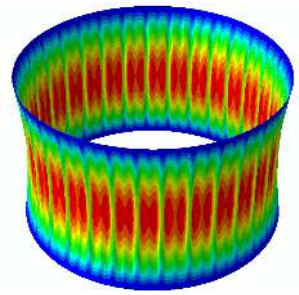

FIGURE 1: CYLINDRICAL MEMBRANE UNDER AXIAL AND PRESSURE LOADS - Magnitude displacement [2].

The membrane is loaded with a steady pressure which represent a first approximation of the pressure due to fluid-structure coupling. Under these representative loads, the membrane structure wrinkles as the result of compressive hoop stress and large topological changes occur at the fluid-structure interface (Fig. 1). In order to circumvent numerical difficulties associated to the singular stiffness matrix, the solution is computed with a quasi-static analysis by means of a dynamic implicit analysis (the structure is slowly loaded) with Hilber Hugues Taylor method. Two types of wrinkles can be clearly observed: principal wrinkles and a set of secondary wrinkles between these primary wrinkles.

FLUID FLOW MODEL

First simulations, involving pre-deformed structures, have shown that the fluid can reasonably be modeled by using a potential flow model to obtain the pressure level at the fluid-structure interface. This result has been obtained by comparing pressures from a RANS simulation to those obtained with a potential flow solver. Moreover, vortices are localized near cylinder extremities where the membrane is highly stiffened by rigid circular rings, reducing the fluid effect. In our approach, the potential problem is solved by using an in-house Fast Boundary Element Method based on the ScalFMM library [3] (Fast Multipole Method) and the PETSc [4] library (iterative solver).

Potential flow model

Potential flow model describes the velocity field of irrotational ($\mathbf{v} = \nabla\phi$) incompressible perfect fluids [5], using a potential function ϕ. Under these assumptions, conservation laws can be written as follows in the fluid

domain Ω_F:

$$\nabla^2\phi(\mathbf{x},t) = 0, \quad \forall(\mathbf{x},t) \in \Omega_F \times [0,T] \tag{1a}$$

$$\frac{\partial\phi(\mathbf{x},t)}{\partial t} - \mathbf{v}_m(\mathbf{x},t).\nabla\phi(\mathbf{x},t) + \frac{|\nabla\phi(\mathbf{x},t)|^2}{2} + g\mathbf{x}.\mathbf{e}_Z + \frac{p(\mathbf{x},t)}{\rho_F} = \frac{p_0(t)}{\rho_F}, \quad \forall(\mathbf{x},t) \in \Omega_F \times [0,T] \tag{1b}$$

Equation (1a) derives from the mass conservation equation, the fluid flow velocity is completely determined by its kinematics. The Bernoulli equation (1b) derives from momentum conservation equation, written here under its Arbitrary Lagrangian Eulerian form [6] in order to take into account convective terms associated to boundary velocity at the fluid-structure interface ($p_0(t)$ is a spatial constant). If no condition is imposed on the velocity potential ϕ, ϕ is defined up to an additive spatial constant: $\phi(\mathbf{x},t) = \phi^*(\mathbf{x},t) + \phi_0(t)$.

$$\nabla^2\phi^*(\mathbf{x},t) = 0, \quad \forall(\mathbf{x},t) \in \Omega_F \times [0,T] \tag{2a}$$

$$\frac{\partial\phi^*(\mathbf{x},t)}{\partial t} - \mathbf{v}_m(\mathbf{x},t).\nabla\phi^*(\mathbf{x},t) + \frac{|\nabla\phi^*(\mathbf{x},t)|^2}{2} + g\mathbf{x}.\mathbf{e}_Z + \frac{p(\mathbf{x},t)}{\rho_F} = \frac{p_0(t)}{\rho_F} - \frac{\partial\phi_0(t)}{\partial t} = c_0(t), \quad \forall(\mathbf{x},t) \in \Omega_F \times [0,T] \tag{2b}$$

$c_0(t)$ can be fixed by imposing the pressure level at one point $\mathbf{x}_0$ in the fluid domain.

Boundary integral equation

Potential problem, described by Equation (1a), can be written as a boundary integral equation [7]. Boundary integral formulations make possible to reduce physical values description in the domain to physical quantities description at the boundary. In the case of an internal flow problem, boundary integral formulation of the potential problem (1a) can be written as follows:

$$\oint_{\partial\Omega} \frac{\partial\phi(\mathbf{y})}{\partial\mathbf{n}(\mathbf{y})} G(\mathbf{x},\mathbf{y})\, dS(\mathbf{y}) - \oint_{\partial\Omega} \phi(\mathbf{y}) \frac{\partial G(\mathbf{x},\mathbf{y})}{\partial\mathbf{n}(\mathbf{y})} dS(\mathbf{y}) = \begin{cases} 0, & \forall\mathbf{x} \in \bar{\Omega}_F \\ \phi(\mathbf{x}), & \forall\mathbf{x} \in \Omega_F \\ \phi(\mathbf{x})/2, & \forall\mathbf{x} \in \partial\Omega_F \end{cases} \tag{3}$$

where $G(\mathbf{x},\mathbf{y}) = 1/4\pi\|\mathbf{x}-\mathbf{y}\|$ is the fundamental solution associated to Laplace's problem [7] and $\partial\Omega_F$ denotes the fluid domain boundary. For the physical problem at stake, boundary description makes easier the management of large topological changes of the fluid domain and facilitates the transfer of physical quantities between fluid and structure sub-problems to enforce spatial coupling conditions.

Numerical methods

By using a collocation method, standard Boundary Element Method (BEM) leads to a linear system with a non-symmetric fully populated operator: $Ax = b$. The operator construction requires $O(N^2)$ operations (where N is the number of unknowns) and its storage has $O(N^2)$ complexity. The linear system is usually solved by means of direct solvers which have $O(N^3)$ complexity. Hence, standard BEM is generally inefficient for large-scale problems despite the dimension reduction associated to the Boundary Integral Equation formulation. The potential problem is then solved by means of fast multipole BEM based on the use of iterative Krylov-based solvers (such as GMRes) and the Fast Multipole Method (FMM) which is used to speed up matrix-vector multiplication during Krylov sub-spaces construction. The use of FMM enables the solver to compute the solution without building explicitly the operator A. FMM is used to assess the influence of far elements whereas near elements contributions are taken into account by means of the standard BEM:

$$\oint_{\partial\Omega} \frac{\partial\phi}{\partial\mathbf{n}} G dS = \oint_{\partial\Omega_{Near}} \frac{\partial\phi}{\partial\mathbf{n}} G dS + \oint_{\partial\Omega_{Far}} \frac{\partial\phi}{\partial\mathbf{n}} G dS \tag{4a}$$

$$\oint_{\partial\Omega} \phi \frac{\partial G}{\partial\mathbf{n}} dS = \oint_{\partial\Omega_{Near}} \phi \frac{\partial G}{\partial\mathbf{n}} dS + \oint_{\partial\Omega_{Far}} \phi \frac{\partial G}{\partial\mathbf{n}} dS \tag{4b}$$

An *octree* structure is computed in order to build a proximity relation between elements and to store multipole and local expansions (values set at cell centers) for each

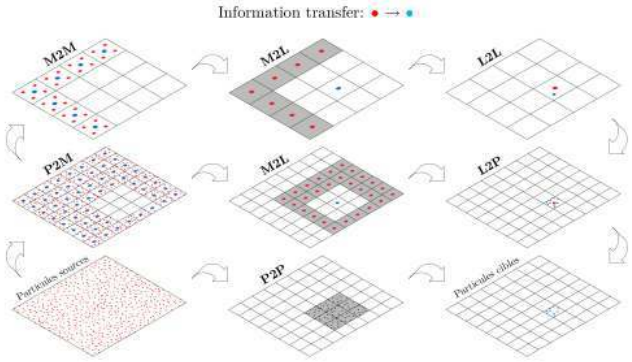

FIGURE 2: FMM PROCEDURE FOR A TWO-DIMENSIONAL DOMAIN [8].

Fast multipole is a three steps procedure. First, element data are transferred to upper levels at multipole expansion points (Upward Pass) by using P2M (Particle To Multipole) and M2M (Moment To Moment) procedures. Then data are localized near each element at local expansion points (Downward Pass) by using M2L (Moment To Local) and L2L (Local To Local) procedures. Integrals are finally computed by means of L2P (Local To Particle) and P2P (Particle To Particle) procedures. In our code, we have considered a spherical kernel for P2M, M2M, M2L, L2L and L2P [9]. Our in-house Fast-BEM code is based on ScalFMM which is a generic parallel fast multipole library [3] and on the GMRes solver available in the PETSc library [4]. ScalFMM has been initially developed to solve point particles problems when the potential decays like 1/r such as electrostatic or gravitational interaction problems. As M2M, M2L, L2L and L2P [9]procedures are available for potential problems in ScalFMM [3], we only have implemented P2M and P2P procedures [9] to adapt the library to integral equations.

Code validations

Our in-house potential solvers (Standard BEM and Fast-BEM codes) are validated by comparing potential results obtained with a finite element code (using a thermal analogy between potential fluid flow and linear heat conduction problems) and our in-house codes on a representative case of the problem at stake. Boundary conditions of the current problem are: zero normal velocity on lateral surfaces and unit normal velocity at top and bottom extremities (Fig. 3).

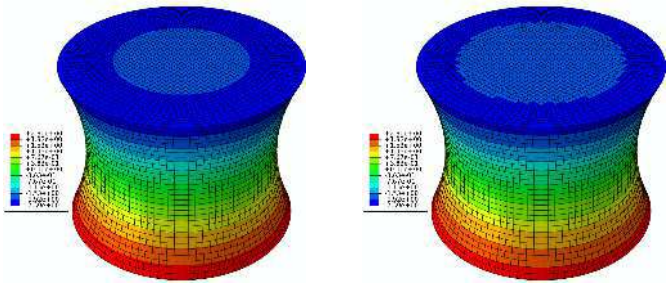

FIGURE 3: IN-HOUSE POTENTIAL CODE VALIDATION (left: FEM model, right: BEM model) - Velocity potential field ϕ $\left[m^2/s\right]$.

Our FastBEM code is validated by comparing potential results obtained with our in-house standard BEM solver and our in-house code on a wrinkled membrane. Boundary conditions of the current problem are: zero normal velocity on lateral surfaces, zero velocity potential on the top end cap and a normal velocity of 1,5 m/s at on the top end cap (Fig. 4).

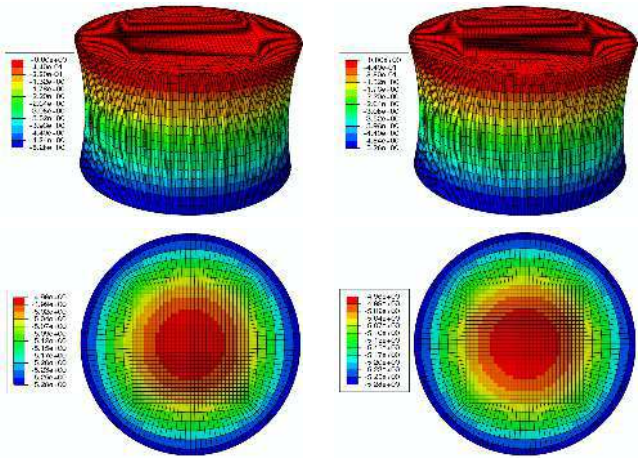

FIGURE 4: IN-HOUSE Fast-BEM CODE VALIDATION (left: BEM, right: Fast-BEM, top: global, bottom: bottom end cap) - Velocity potential field ϕ $\left[m^2/s\right]$.

COUPLED MODEL

The fluid-structure coupling is achieved by means of the ABAQUS® Co-Simulation Engine allowing the user to couple ABAQUS® solvers with a third-party solver. At the fluid-structure interface, kinematic and dynamic coupling conditions are imposed which represent normal velocity (Eqn. 5a) and normal stress continuity (Eqn. 5b)

at the interface, repectively.

$$\mathbf{v}_F(\mathbf{x}).\mathbf{n}(\mathbf{x}) = \frac{d\mathbf{u}_S(\mathbf{x})}{dt}.\mathbf{n}(\mathbf{x}) \tag{5a}$$

$$\left(\sigma^S(\mathbf{x}).\mathbf{n}\right).\mathbf{n} = \left(\sigma^F(\mathbf{x}).\mathbf{n}\right).\mathbf{n} \tag{5b}$$

The Co-Simulation Engine is in charge of i) the spatial mapping in order to transfer physical quantities between each sub-model mesh and ii) the time coupling scheme in order to synchronize each solver call. Available time coupling schemes are rather standard: Conventional Serial Staggered or Conventional Parallel Staggered schemes [10] and Jacobi [11] or Gauss-Seidel [12] iterative schemes. CSS and CPS schemes are appropriate to solve problems with weak physical coupling, whereas the last two ones should be used to assess the solution of moderately coupled problems. Iterative time coupling schemes can be improved using relaxation method [13,14], Interface Block Quasi Newton methods [3,15] or Interface Quasi Newton algorithms [16,17].

Time coupling scheme

We use the same mesh for fluid and structure subproblems, hence physical quantity mapping is relatively trivial. The problem of thin and light structures coupled with heavy fluids requires a strong numerical coupling schemes. In order to ensure such a coupling, standard iterative time coupling schemes available in ABAQUS® CSE is enhanced using relaxation method or efficient Interface Quasi-Newton algorithms which speed up the coupling scheme convergence.

Relaxation method The relaxation method involving dynamic relaxation parameters consists in predicting the structural displacement ($\mathbf{u}_{k+1}^{P,n+1}$) by correcting the computed displacement ($\mathbf{u}_{k+1}^{n+1}$) with the previous displacement prediction ($\mathbf{u}_k^{P,n+1}$):

$$\mathbf{u}_{k+1}^{P,n+1} = \omega_k \mathbf{u}_{k+1}^{n+1} + (1-\omega_k)\,\mathbf{u}_k^{P,n+1} \tag{6}$$

where $n+1$ and k are the current time increment and the current iteration indices and the dynamic relaxation parameter ω_k is assessed by Aitken method [13].

Interface Quasi Newton algorithms Interface Quasi Newton algorithms focus on the residual interface displacement:

$$\mathbf{r}(\mathbf{u}) = S \circ F(\mathbf{u}) - \mathbf{u} = 0 \tag{7a}$$

$$\Delta\mathbf{u} = -\left(\frac{\partial \mathbf{r}}{\partial \mathbf{u}}\right)^{-1} \mathbf{r}(\mathbf{u}) \tag{7b}$$

where S and F are the structural and fluid solver, respectively. These algorithms are used to make a relevant fluid-structure interface displacement prediction using a numerically evaluated tangent matrix of the interface displacement built during the iterative procedure.

Validation case

The coupling procedure has been firstly validated by coupling ABAQUS® and an in-house standard boundary element solver. The validation is made on the case of a free spring/sphere-shaped mass system immersed in a fluid and where the mass is initially shifted ($m = 155kg$, $k = 10000Nm^{-1}$).

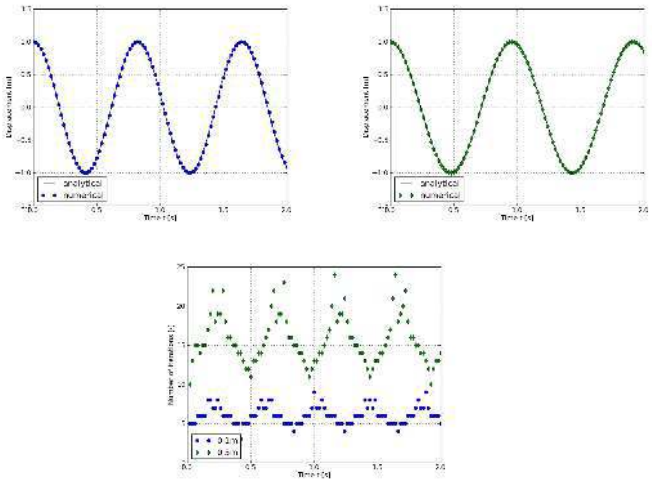

FIGURE 5: COUPLING PROCEDURE VALIDATION - SPRING/SPHERE-SHAPED MASS.

The first figure (in Fig.5) and the second figure (in Fig.5) represent the mass displacement response for an added mass of 10% (blue) and 50% (green) of the structural mass, respectively. The third figure (in Fig.5) represents the number of iterations during the computation procedure.

Case of interest

The case of interest is a very long and highly flexible immersed circular cylinder with an internal flow under axial force and fluid-structure interaction loadings. The global behavior of the structure is computed by means of a one-dimensional solvers. The local behavior of the structure is assessed with a three-dimensional analysis with fluid-structure interaction modeling of a small part of the global structure. Problem dimensions and material properties are given without any dimensions with respect to $L* = R$ (caracteristic length), $t* = (\rho_S R^2/E)^{0.5}$ (caracteristic time) and $p* = E$ (caracteristic pressure). Dimensions, material properties and permanent loads of the three-dimensional problem are given in Tab.1.

Physical value	Symbol	Expression	Value
Cylinder radius	$\overline{R}$	R/R	1.00
Cylinder length	$\overline{h}$	h/R	$8.00\ 10^{-01}$
Shell thickness	$\overline{e}$	e/R	$4.30\ 10^{-04}$
Fluid density	$\overline{\rho}_F$	ρ_F/ρ_S	1.00
Structural density	$\overline{\rho}_S$	ρ_S/ρ_S	1.00
Yound modulus	$\overline{E}$	E/E	1.00
Axial force	$\overline{T}$	T/ER^2	$7.40\ 10^{-05}$
Pressure	$\overline{p}$	p/E	$4.00\ 10^{-06}$

TABLE 1: DIMENSION, MATERIAL PROPERTIES & PERMANENT LOADS.

Structure and fluid boundary conditions Structural and fluid boundary conditions at submodel interfaces (in terms of effort/kinematics and fluid velocity/pressure, respectively) are given by one-dimensional simulations. The cylindrical structure is pre-loaded with a permanent axial load and a permanent pressure Tab.1

Boundary conditions for internal and external fluid sub-problems are i) an uniform inlet velocity $v_{in}(x_0,t)$ and an imposed pressure $p(x_0,t)$ at point x_0 on the fluid-structure interface. Furthermore, a parallel flow assumption is formulated at the outlet in order to let the fluid flow. Figure 6 summurizes boundary conditions imposed on fluid domain boundaries:

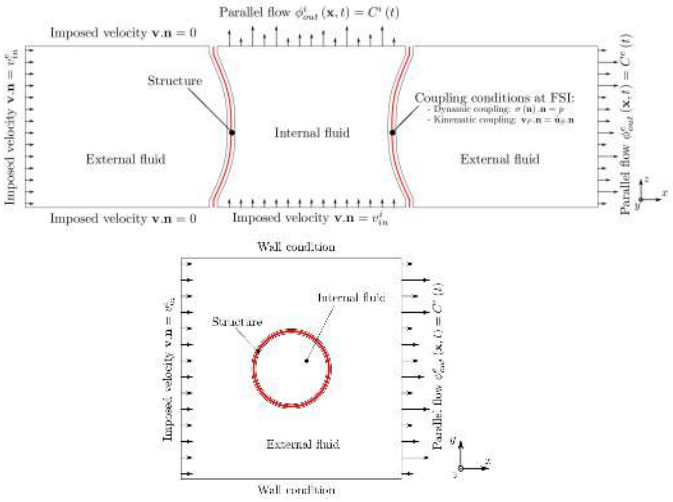

FIGURE 6: BOUNDARY CONDITIONS FOR THE INTERNAL AND EXTERNAL FLUID SUB-PROBLEMS.

The imposed velocity at the inlet of the exterior fluid problem is assumed to be zero. At the outlet a parallel flow is modeled (*i.e.*, zero tangential fluid velocity) by imposing a constant potential fluid velocity on the boundary. Inlet fluid velocity (Fig. 7) for the internal problem is obtained by means of a one-dimensional Fluid-Structure Interaction solver:

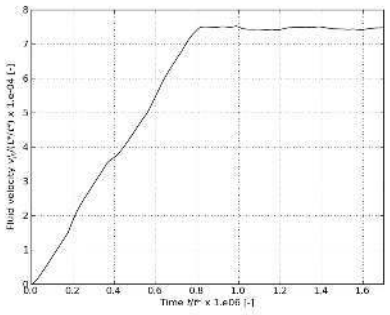

FIGURE 7: IMPOSED FLUID VELOCITY FOR THE INTERNAL FLUID FLOW.

The one-dimensional solver provides a resultant pressure load ($p^{ext} - p^{int}$). This pressure (Fig. 8) is imposed during fluid sub-problems resolution in order to set potential fluid problem constants.

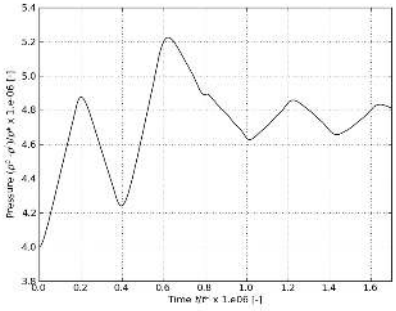

FIGURE 8: REFERENCE PRESSURE FOR THE FLUID FLOW PROBLEM.

Permanent loads, *i.e.* axial force and static pressure (pressure at time $\bar{t} = 0$), are imposed to a purely structural model in a first quasi-static analysis. The bottom extremity is clamped. The quasi-static analysis allows us to circumvent numerical difficulties associated to the singular stiffness matrix by taking into account mass matrix contribution in the tangent matrix. The coupled analysis is then started from this pre-deformed and pre-stressed state and performed by means of a co-simulated analysis between ABAQUS and our in-house fluid solver. Inlet velocity and reference pressure are imposed to the fluid model.

Results In a first approach, the external fluid is neglected and only the fluid-structure interaction between the internal fluid and the tructure is taken into account. In order to reach the convergence and since dynamic loads are quite smooth, structural mass is artificially increased. Figure 9 shows the initial radial displacement field at time $\bar{t} = 0$ (due to permanent loads) and the final radial displacement field at time $\bar{t} = 1.7$:

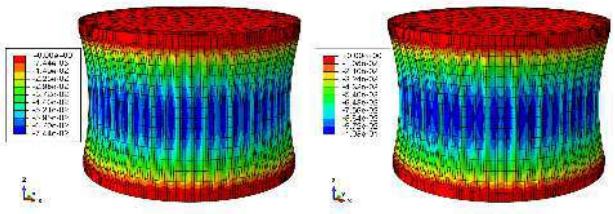

FIGURE 9: RADIAL DISPLACEMENT. *Radial displacement at time $\bar{t} = 0$ (on the left) and $\bar{t} = 1.7$ (on the right).*

The top extremity of the structure is loaded with an axial force and is free to move when the structure is subjected fluid-structure interaction loadings. Figure 10 shows the axial displacement of the top extremity.

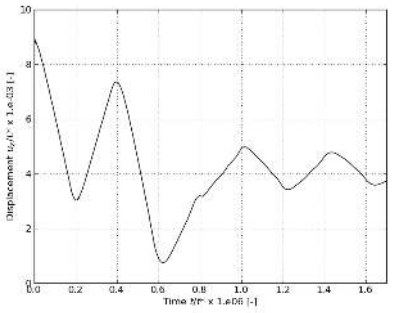

FIGURE 10: AXIAL DISPLACEMENT OF THE TOP EXTREMITY - TIME HISTORY.

Pressure in the fluid domain is computed at the fluid-structure interface by means of an in-house potential solver. Figure 11 shows the pressure field at the end of the analysis. As expected, we can notice that the pressure level is higher at $h/2$ due to the fluid acceleration associated with the section reduction

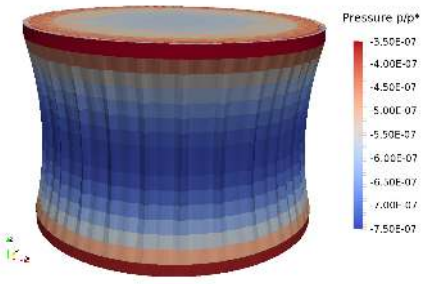

FIGURE 11: PRESSURE FIELD AT THE FLUID-STRUCTURE INTERFACE AT TIME $\overline{T} = 1.7$.

Figure 12 shows the pressure time history for different altitudes.

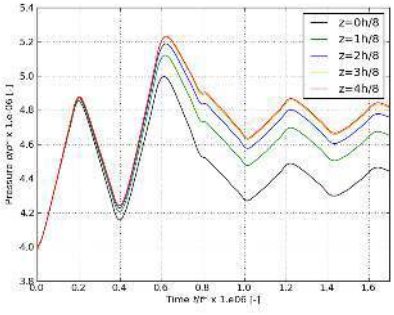

FIGURE 12: PRESSURE AT DIFFERENT ALTITUDES.

WORK IN PROGRESS

Taking into account external fluid domain will probably allow us to reduce the artificial structural mass since it is expected to compensate internal fluid-structure interaction loadings. Hence, our effort are focused on taking into account external fluid flow effect. In order to validate the global numerical procedure we use for designing the structure, physical experiments are moreover in progress. In particular, these experiments will be analyzed in order to validate one-dimensional solvers and the three-dimensional analysis by a submodeling approach.

REFERENCES

[1] Dassault Systèmes, Providence, R. U., 2014. *ABAQUS - ABAQUS Documentation*.

[2] Bouzidi, R., and Véron, E., 2015. "Solution semi-analytique de la déformée d'une structure membranaire de forme cylindrique circulaire sous pression externe en grandes transformations". In 12ème Colloque National en Calcul des Structures.

[3] Blanchard, P., Bramas, B., Olivier, C., Darve, E., Dupuy, L., Etcheverry, A., and Sylvand, G., 2015. "Scalfmm: A generic parallel fast multipole library". In Proceedings of Computational Science and Engineering (CSE) 2015.

[4] Balay, S., Gropp, W., Curfman McInnes, L., and Smith, B., 1997. *Efficient Management of Parallelism in Object Oriented Numerical Software Libraries - Chap. 8: Modern Softwre Tools in Scientific Computing , pp. 163–202.* Birkhauser.

[5] Chassaing, P., 2010. *Mécanique des fluides - Elément d'un premier parcours*. Cépaduès.

[6] Nitikitpaiboon, C., and Bathe, K.-J., 1993. "An arbitrary lagrangian-eulerian velocity potential formulation for fluid-structure interaction". *Computers & Structures,* ***47***, pp. 871–891.

[7] Bonnet, M., 1999. *Boundary integral equation methods for solids and fluids*. Wiley.

[8] Yokota, R., and Barba, L. A., 2011. *Treecode and fastmultipole method for N-body simulation with CUDA: Chapitre 9 de "GPU Computing Gems"*. Morgan Kauffmann: 1st edition.

[9] Liu, Y., 2009. *Fast Multipole Boundary Element Methods: Theory and Applications in Engineering*. Society for Industrial an Applied Mathematics.

[10] Piperno, S., Farhat, C., and Larrouturou, B., 1995. "Partitioned procedures for the transient solution of coupled aeroelastic problems - part i: Model problem, theory and two-dimensional application". *Computer Methods in Applied Mechanics and Engineering,* ***124***, pp. 79–112.

[11] Barrett, R., Berry, M., Chan, T., Demmel, J., Donato, J., Dongarra, J., Eijkhout, V., Pozo, R., Romine, C., and Van der Vorst, H., 2001. *Templates for the Solution of Linear Systems: Building Blocks for Iterative Methods*. Society for Industrial an Applied Mathematics.

[12] Wood, C., Gil, A., Hassan, O., and Bonet, J., 2010. "Partitioned block-gauss-seidel coupling for dynamic fluid-structure interaction". *Computers & Structures,* ***88***, pp. 1367–1382.

[13] Küttler, U., and Wall, W., 2008. "Fixed-point fluid-structure interaction solvers with dynamic relaxation". *Computational Mechanics,* ***43***, pp. 61–72.

[14] Yvin, C., 2014. "Interaction fluide-structure pour des configurations multi-corps. Applications aux liaisons complexes, lois de commande d'actionneur et systmes souples dans le domaine maritime". PhD Thesis, LHEEA - Laboratoire de recherche en Hydrodynamique, nergtique et Environnement Atmosphrique, December.

[15] Bogaers, A., Kok, S., Reddy, B., and Franz, T., 2014. "Quasi-newton methods for implicit black-box fsi coupling". *Computer Methods in Applied Mechanics and Engineering,* ***279***, pp. 113–132.

[16] Michler, C., Van Brummelen, H., and De Borst, R., 2011. "An investigation of interface-gmres(r) for fluid-structure interaction problems with flutter and divergence". *Computational Mechanics,* ***47***, pp. 17–29.

[17] Vierendeels, J., Lanoye, L., Degroote, J., and Verdonck, P., 2007. "Implicit coupling of partitioned fluid-structure interaction problems with reduced order models". *Computers & Structures,* ***85***, pp. 970–976.